

# Intrinsic Proton-Donating Power of Zinc-Bound Water in a Carbonic Anhydrase Active Site Model Estimated by NMR

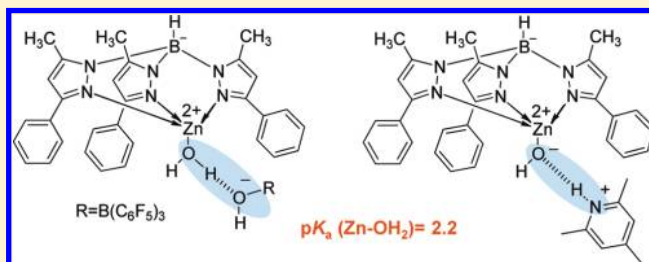
Stepan B. Lesnichin,<sup>†,‡</sup> Ilya G. Shenderovich,<sup>\*,†,‡</sup> Titin Muljati,<sup>†,§</sup> David Silverman,<sup>||</sup> and Hans-Heinrich Limbach<sup>\*,†</sup>

<sup>†</sup>Institut für Chemie und Biochemie, Freie Universität Berlin, Takustrasse 3, 14195, Berlin, Germany

<sup>‡</sup>Department of Physics, St. Petersburg State University, Ulianovskaja 3, 198504 St. Petersburg, Russia

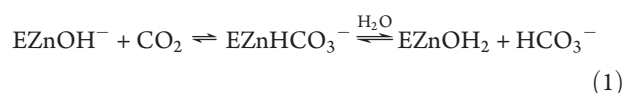
<sup>||</sup>Departments of Pharmacology and Therapeutics, and Biochemistry and Molecular Biology, College of Medicine, University of Florida, Gainesville, Florida 32610, United States

**ABSTRACT:** Using liquid-state NMR spectroscopy we have estimated the proton-donating ability of Zn-bound water in organometallic complexes designed as models for the active site of the metalloenzyme carbonic anhydrase (CA). This ability is important for the understanding of the enzyme reaction mechanism. The desired information was obtained by <sup>1</sup>H and <sup>15</sup>N NMR at 180 K of solutions of [Tp<sup>Ph,Me</sup>ZnOH] (**1**, Tp<sup>Ph,Me</sup> = tris(2-methyl-4-phenylpyrazolyl)hydroborate) in CD<sub>2</sub>Cl<sub>2</sub>, in the absence and presence of the proton donors (C<sub>6</sub>F<sub>5</sub>)<sub>3</sub>BOH<sub>2</sub> [aquatris(pentafluorophenyl)boron] and Col-H<sup>+</sup> (2,4,6-trimethylpyridine-H<sup>+</sup>). Col-H<sup>+</sup> forms a strong OHN hydrogen bond with **1**, where the proton is located closer to nitrogen than to oxygen. (C<sub>6</sub>F<sub>5</sub>)<sub>3</sub>BOH<sub>2</sub>, which exhibits a pK<sub>a</sub> value of 1 in water, also forms a strong hydrogen bond with **1**, where the proton is shifted slightly across the hydrogen-bond center toward the Zn-bound oxygen. Finally, a complex between Col and (C<sub>6</sub>F<sub>5</sub>)<sub>3</sub>BOH<sub>2</sub> was identified, exhibiting a zwitterionic OHN hydrogen bond, where H is entirely shifted to nitrogen. The comparison with complexes of Col with carboxylic acids studied previously suggests that, surprisingly, the Zn-bound water exhibits in an aprotic environment a similar proton-donating ability as a carboxylic acid characterized in water by a pK<sub>a</sub> of 2.2 ± 0.6. This value is much smaller than the value of 9 found for [Zn(OH<sub>2</sub>)<sub>6</sub>]<sup>2+</sup> in water and those between 5 and 8 reported for different forms of CA. Implications for the biological function of CA are discussed.



## INTRODUCTION

Carbonic anhydrase (CA) is a widely occurring metalloenzyme found in animals, plants, certain bacteria, and viruses.<sup>1–3</sup> The physiological function of this enzyme is to catalyze the reversible hydration of CO<sub>2</sub>, producing HCO<sub>3</sub><sup>–</sup> and H<sub>3</sub>O<sup>+</sup> as well as the reverse reaction.<sup>4</sup> Most of the forms of human CA contain in the active site an essential zinc ion, Zn<sup>2+</sup>, to which either a water molecule or the corresponding hydroxide base is bound.<sup>5</sup> The catalytic cycle of CA (or E ≡ enzyme) is considered to involve two main steps:<sup>6</sup>



and



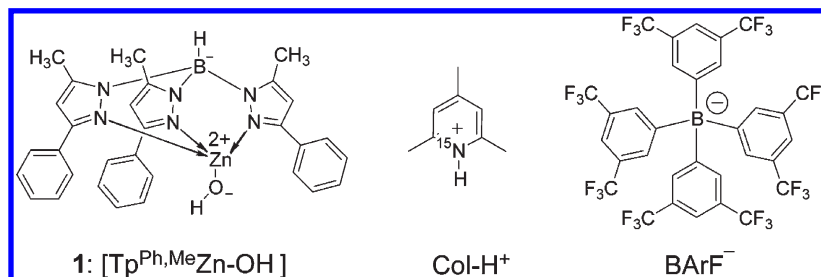
where B represents the imidazole residue of a nearby histidine side chain (His64) which carries the proton to aqueous solution.<sup>2,7–13</sup> This proton transfer is believed to be the rate-limiting step of the catalytic cycle and is conventionally treated as a reaction in aqueous solution. As His64 is located about 7 Å away from Zn it has been suggested that the proton is transferred

to the base via a network of hydrogen-bonded water molecules. This hypothesis has motivated a number of studies of the role of water in the active site.<sup>14–18</sup> The analysis of pH-dependent kinetic reaction profiles led to the conclusion that the pK<sub>a</sub> value of Zn-bound water in human CA II varies between 6 and 7,<sup>2,6</sup> similar to that of the imidazole residue of His64. A smaller value was found in the case of the isozyme III.<sup>19,20</sup> By contrast, [Zn(OH<sub>2</sub>)<sub>6</sub>]<sup>2+</sup> exhibits in aqueous solution a pK<sub>a</sub> value of 9.<sup>21</sup> This wide acidity range has initiated an intensive search for molecular species feasible to mimic the acid–base properties of Zn-bound water in CA.<sup>21–25</sup> Indeed, several model systems have been observed that exhibit in aqueous solution a pK<sub>a</sub> between 6 and 7. Thus, the enzyme apparently increases the proton donor ability of Zn-bound water.

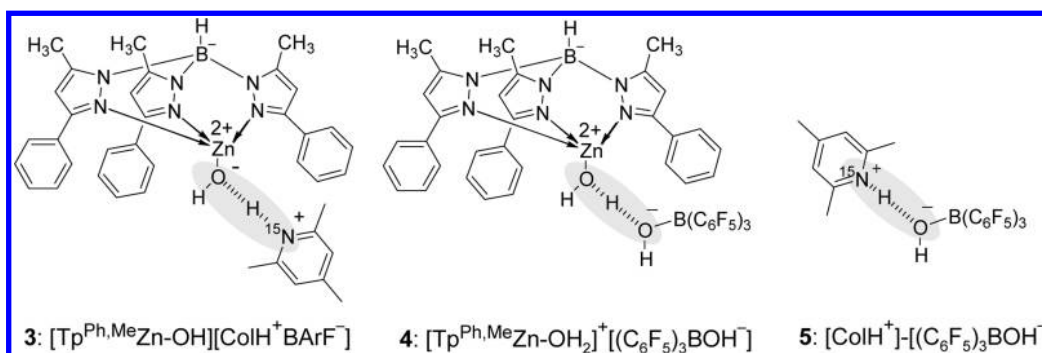
However, the question arises whether the rules that govern acid–base properties in water are maintained in the active sites of enzymes. In contrast to aqueous solution, zinc-bound water in CA is mainly surrounded by the protein matrix with just a few water molecules inside the active site.<sup>7,26</sup> In such cases, the proton-donating abilities may depend on the local environment.<sup>26,27</sup> To our knowledge, the intrinsic proton-donating ability of Zn-bound

Received: April 15, 2011

Published: June 20, 2011

Scheme 1. Organometallic CA Active Site Model 1 and Col-H<sup>+</sup> BARF<sup>-</sup>

Scheme 2. Hydrogen-Bonded Complexes 3–5



water in a suitable model environment has not yet been established experimentally. Evidence has been obtained in the case of aspartate aminotransferase that acid–base interactions in the active site are better modeled using polar organic solvents rather than using aqueous solutions.<sup>28</sup> Thus, to contribute to our understanding of the proton-donating ability of the zinc-bound water in the active site of CA we undertook the present NMR study of organometallic model systems at 180 K in the presence of acids using CD<sub>2</sub>Cl<sub>2</sub> as solvent, which exhibits at this temperature a dielectric constant of about 16.<sup>29,30</sup>

Various model systems have been proposed to mimic the active site of CA. Among them are macrocyclic aliphatic polyamine complexes with Zn<sup>2+</sup> designed by Kimura et al.<sup>25</sup> for studies in aqueous solution. These complexes carry a positive charge as Zn in CA. The present study was devoted to neutral tris-(pyrazolyl)hydroborate zinc hydroxide complexes of the type [Tp<sup>R<sub>1</sub>,R<sub>2</sub></sup>ZnOH] designed by Vahrenkamp and Trofimenko.<sup>31–34</sup> The advantage of these complexes is that they are soluble in some polar organic solvents, which seems to better mimic the electrostatic properties of enzymic acid sites than aqueous solutions.<sup>28</sup> As these complexes are not soluble in water, their pK<sub>a</sub> values could not be measured directly but only estimated to be smaller than 7.<sup>32,33,21</sup> Two complexes, **1** with R<sub>1</sub> = phenyl and R<sub>2</sub> = methyl, [Tp<sup>Ph,Me</sup>ZnOH] (Scheme 1), and **2** with R<sub>1</sub> = *tert*-butyl and R<sub>2</sub> = methyl, [Tp<sup>*t*-Bu,Me</sup>ZnOH], have been mainly studied, but these studies were complicated by the following. In the case of **2**, the characteristic hydroxide signal could be observed at  $-0.06$  ppm,<sup>31</sup> but this was due to the presence of the bulky substituents which also hindered the interaction of [ZnOH] with proton donors. Such an interaction was present in the case of **1**, but the hydroxide signal could not be observed because of fast proton exchange with residual water. Here we choose to study **1**, as we wanted to study specifically this interaction. The proton exchange problem of **1**

was solved in this study by performing NMR experiments at 180 K, where the amount of residual water was reduced and proton exchange was slower than at room temperature.

In order to find a suitable system which could mimic the acid–base properties of His64 in CA we searched among <sup>15</sup>N-enriched pyridine derivatives which have been frequently used to study hydrogen bonding by NMR.<sup>35–37</sup> One of the most studied derivatives is 2,4,6-trimethylpyridine (collidine, Scheme 1), for which correlations between hydrogen bond geometries and NMR parameters have been established.<sup>37,38</sup> Its protonated form exhibits a pK<sub>a</sub> value of 7.4,<sup>39</sup> which is very similar to the value of 7.35 found for 4-methylimidazole-H<sup>+</sup>.<sup>40</sup> We anticipated that collidinium could form a hydrogen-bonded complex **3** with **1** using a suitable counteranion such as the noncoordinating anion tetrakis[3,5-bis(trifluoromethyl)phenyl] borate B[C<sub>6</sub>H<sub>3</sub>(CF<sub>3</sub>)<sub>2</sub>]<sub>4</sub><sup>-</sup> (BARF<sup>-</sup>, Scheme 1).<sup>41,42</sup> The structure of the resulting acid–base complex is depicted in Scheme 2, whose <sup>1</sup>H and <sup>15</sup>N NMR parameters we studied here in order to obtain information about the relative proton-donating abilities. We also explored the use of the less acidic 4-(*N,N*-dimethylamino)pyridinium (DMAP-H<sup>+</sup>) but found that the latter forms a covalent Zn–N bond.

For comparison, we also studied complex **4**, formed by **1** with tris(perfluorophenyl)boron ([C<sub>6</sub>F<sub>5</sub>]<sub>3</sub>BOH<sub>2</sub>] ≡ [BOH<sub>2</sub>]). The latter is the only known strong acid (pK<sub>a</sub> = 0.9<sup>39</sup>) that is able to stabilize [Tp<sup>*t*-Bu,Me</sup>ZnOH<sub>2</sub>]<sup>+</sup>.<sup>43</sup> According to its X-ray crystallographic structure, the resulting complex contains a short OHO hydrogen bond exhibiting an O···O distance of 2.480(3) Å.<sup>43</sup> The treatment of **2** with common strong HX acids (X<sup>-</sup> = Cl<sup>-</sup>, Br<sup>-</sup>, *p*-TsO<sup>-</sup>) leads to either a destruction of **2** or an irreversible conversion of [Tp<sup>*t*-Bu,Me</sup>ZnOH] to [Tp<sup>*t*-Bu,Me</sup>ZnX]. **4** can be considered as a model of the transition state of proton transfer from the Zn-bound water molecule to an adjacent water molecule. Finally, Scheme 2 also depicts the structure of complex **5**

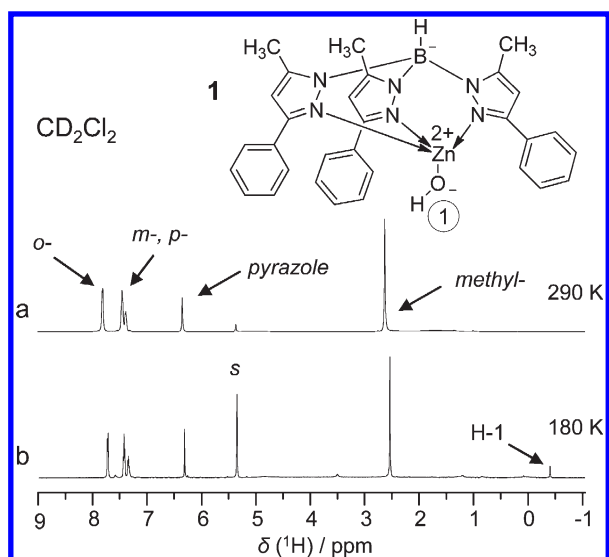


**Figure 1.**  $^1\text{H}$  NMR spectra of  $[\text{Tp}^{\text{Ph,Me}}\text{ZnOH}]$  dissolved in  $\text{CD}_2\text{Cl}_2$  at 290 K (a) and 180 K (b). *S* denotes the solvent.

studied here in order to elucidate the relative proton-donating power of  $[(\text{C}_6\text{F}_5)_3\text{BOH}_2]$  and collidinium.

This paper is organized as follows. After the Experimental Section, the results of our NMR studies of **1**, **3**, **4** and **5** in aprotic polar solution will be described and then discussed with respect to the proton-donating ability of the Zn-bound water in CA.

## EXPERIMENTAL SECTION

**Compounds.**  $\text{CD}_2\text{Cl}_2$  (99.6% D) was purchased from Eurisotop GmbH, Germany. All other chemicals were purchased from Sigma-Aldrich and were used without additional purification.

$^{15}\text{N}$ -labeled pyridine, 4-methylpyridine, 2,4,6-trimethylpyridine (hereafter Col), and 4-(*N,N*-dimethylamino)pyridine (hereafter DMAP) were synthesized as described previously.<sup>44–46</sup>  $[\text{Tp}^{\text{Ph,Me}}\text{ZnOH}]$  was a gift of H. Vahrenkamp (Freiburg, Germany). It was synthesized and characterized by  $^1\text{H}$  NMR as described previously by Ruf et al.<sup>32</sup>

$[(\text{C}_6\text{F}_5)_3\text{BOH}_2]$  was prepared as follows. A 1.0  $\mu\text{L}$  portion of  $\text{H}_2\text{O}$  (0.056 mmol) was added into a solution of  $(\text{C}_6\text{F}_5)_3\text{B}$  (28 mg, 0.055 mmol) in pentane (6 mL). The mixture was stirred for 2 h and then filtered. The precipitate was washed two times with pentane (5 mL) and dried under vacuum over 30 min, giving  $[(\text{C}_6\text{F}_5)_3\text{BOH}_2]$  as a white solid (21.4 mg, 73% yield). IR data (KBr,  $\text{cm}^{-1}$ ):  $\nu_{\text{OH}} = 3510$  (m), 3396 (br).

$^{15}\text{N}$ -labeled  $\text{ColH}^+ \text{BARF}^-$  was prepared as follows.  $\text{Na}^+ \text{BARF}^-$  was synthesized according to the procedure reported by Brookhart et al.<sup>41</sup> and modified by Gründemann.<sup>47</sup> A 5  $\mu\text{L}$  portion of  $^{15}\text{N}$ -labeled collidine (38 mmol) and 3.5 mL of 37% water solution of HCl (41.8 mmol) were dissolved in 2 mL of water and stirred for 15 min. Then 37.0 mg of  $\text{Na}^+ \text{BARF}^-$  (41.8 mmol) was added. The mixture was vigorously stirred over several hours, forming the yellowish-white flakes of  $^{15}\text{N}$ -labeled  $\text{ColH}^+ \text{BARF}^-$ . The precipitate was filtrated, washed with water, and dried under vacuum overnight.

**NMR Spectroscopy.** NMR spectra were recorded on a Bruker AMX-500 instrument operating at 11.7 T. An Eurothermic variable temperature unit was used to adjust temperatures with an accuracy of  $\pm 1$  K.  $^1\text{H}$  NMR chemical shifts were referenced relative to  $\text{CH}_2\text{Cl}_2$ ,  $\delta$  ( $^1\text{H}$ ) = 5.3 ppm. The  $^{15}\text{N}$  chemical shifts of DMAP and of Col with respect to solid  $^{15}\text{NH}_4\text{Cl}$  are 236 and 268 ppm, respectively.<sup>48,37</sup>

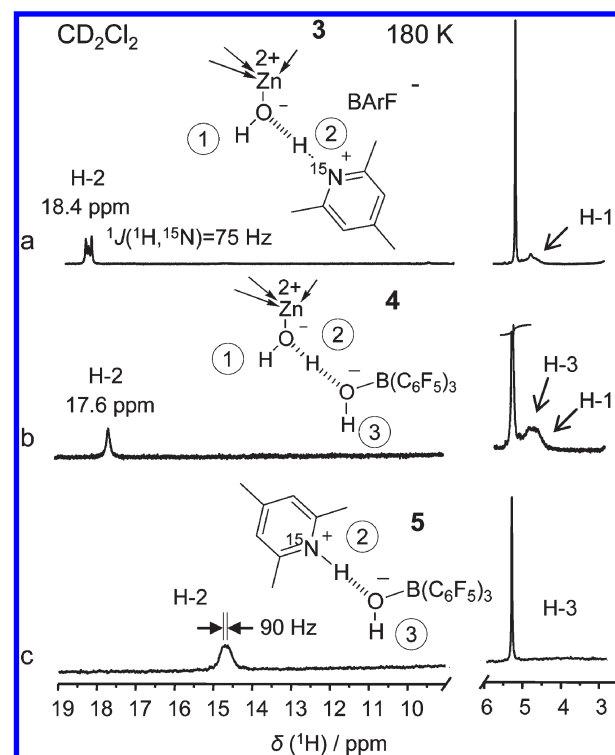


**Figure 2.** Partial  $^1\text{H}$  NMR spectra at 180 K of **3** (a), **4** (b), and **5** (c) dissolved in  $\text{CD}_2\text{Cl}_2$ .

## RESULTS

**$^1\text{H}$  NMR Spectroscopy.** In Figure 1 are depicted the  $^1\text{H}$  NMR spectra of **1** dissolved in  $\text{CD}_2\text{Cl}_2$ . At room temperature only signals of nonexchangeable protons are observed as traces of water in  $\text{CD}_2\text{Cl}_2$  promote intermolecular proton exchange. At 180 K, water precipitates from  $\text{CD}_2\text{Cl}_2$  and an additional signal appears at  $-0.5$  ppm. This signal corresponds to a single proton as revealed by signal integration. A similar signal was observed for **2** in  $\text{CD}_2\text{Cl}_2$  at room temperature at  $-0.06$  ppm.<sup>31</sup> These signals arise from the proton of Zn-bound hydroxide. The addition of pyridine, DMAP, or Col to the solution of **1** does not affect the signal at  $-0.5$  ppm.

By contrast, the signal at  $-0.5$  ppm disappears when pyridine- $\text{H}^+ \text{BF}_4^-$ , 4-methylpyridine- $\text{H}^+ \text{BF}_4^-$ , DMAP- $\text{H}^+ \text{BF}_4^-$ , or Col- $\text{H}^+ \text{BF}_4^-$  is added to the solution of **1** in  $\text{CD}_2\text{Cl}_2$ . However, no other signals appear in the  $^1\text{H}$  NMR spectra down to 180 K, which could be assigned to mobile protons. Presumably, these protons are involved in an intermolecular exchange. It was not possible to freeze out this exchange by performing NMR experiments at lower temperatures using a  $\text{CDF}_3/\text{CDF}_2\text{Cl}$  mixture which is liquid down to 100 K<sup>30</sup> because of solubility problems.

The situation is different when  $\text{ColH}^+ \text{BARF}^-$  labeled to about 70% with  $^{15}\text{N}$  is added to the solution of **1** in  $\text{CD}_2\text{Cl}_2$ . As depicted in Figure 2a, new signals at 18.4 and 4.7 ppm are present at 180 K. The low-field signal H-2 is split into a doublet by scalar coupling with the  $^{15}\text{N}$  nucleus of Col, exhibiting a coupling constant of  $|^1J(^1\text{H}, ^{15}\text{N})| = 75$  Hz. Because of the incomplete  $^{15}\text{N}$  labeling, a small central peak is present in the spectrum. This peak corresponds to the protons bound to the nonlabeled Col. We assign this signal to an  $\text{O} \cdots \text{H} - \text{N}$  hydrogen bond formed by collidinium with the Zn-bound hydroxide group, i.e., to the formation of **3**. The signal at 4.7 ppm is typical for small water

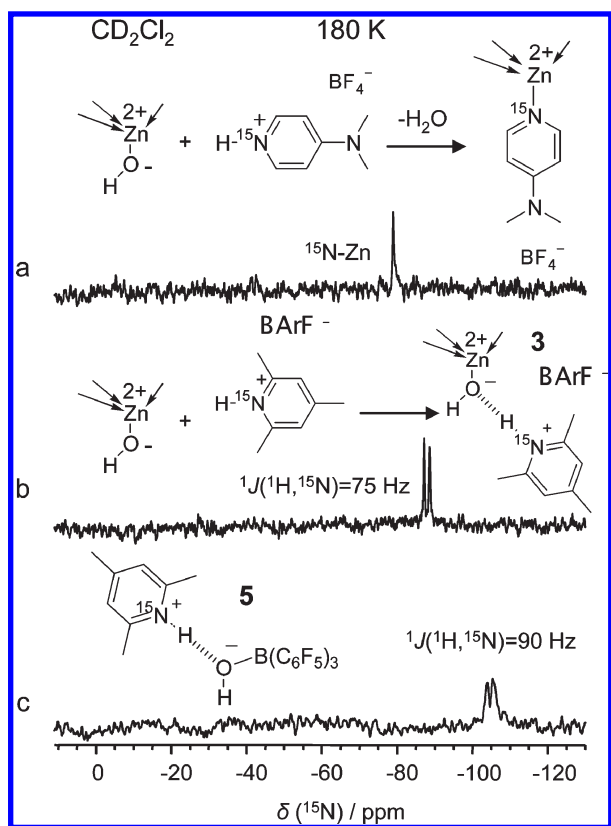


**Figure 3.**  $^{15}\text{N}$  NMR spectra at 180 K of  $[\text{Tp}^{\text{Ph,Me}}\text{Zn}-\text{DMAP}(^{15}\text{N})]^+$  (a), **3** (b), and **5** (c) dissolved in  $\text{CD}_2\text{Cl}_2$ . The chemical shifts are referenced to DMAP (a) and Col (b, c) in  $\text{CD}_2\text{Cl}_2$  (set as 0 ppm).

clusters.<sup>49</sup> Therefore, this signal is assigned to residual water interacting or exchanging protons with H-1 of the  $[\text{ZnOH}]$  group. Note that extreme line broadening arising from intermediate proton exchange rates could lead to a missing signal component of H-1. Would it be possible to perform the measurements at lower temperatures, the residual water molecules freeze out and allow one to determine the intrinsic chemical shift of H-1 precisely, probably around  $-0.5$  ppm.

In order to establish the relative proton-donating ability of Zn-bound water toward a strong oxygen acid, low-temperature  $^1\text{H}$  NMR spectra of a  $\text{CD}_2\text{Cl}_2$  solution of **1** in the presence of  $(\text{C}_6\text{F}_5)_3\text{BOH}_2$  were measured. A typical spectrum is depicted in Figure 2b. Three signals are observed at 180 K, indicating the formation of complex **4**. A singlet at 17.6 ppm is assigned to the bridging proton H-2 of the OHO hydrogen bond. The broad signal at 4.6 ppm is again tentatively attributed to the “outer” protons involved in an interaction and/or exchange with residual water.

Finally, in order to establish the relative proton-donating power of  $\text{ColH}^+$  and of  $(\text{C}_6\text{F}_5)_3\text{BOH}_2$ , a  $^1\text{H}$  spectrum of a 1:1 mixture of both compounds in  $\text{CD}_2\text{Cl}_2$  at 180 K was obtained as depicted in Figure 2c, where  $\text{ColH}^+$  was labeled to about 70% with  $^{15}\text{N}$ . A broad signal is observed at 14.6 ppm, exhibiting a line width of about 300 Hz, which is larger than the expected value of about 90 Hz for  $|^1J(^1\text{H}, ^{15}\text{N})|$ .<sup>27</sup> This signal is assigned to the OHN hydrogen bond of the complex  $[(\text{C}_6\text{F}_5)_3\text{BOH}_2\text{Col}]$  **5**, where the hydrogen-bonded proton must be involved in a moderately fast exchange with another proton exhibiting a different chemical shift. This could be H-3, which on the other

hand will exchange with residual water and hence its signal is lost in the baseline. Note that H-3 is not shielded by bulky phenyl groups as it is in the case of **4**.

**$^{15}\text{N}$  NMR Spectroscopy.** No signals were detected in the  $^{15}\text{N}$  NMR spectra of equimolar solutions of **1** and  $^{15}\text{N}$ -enriched pyridinium, collidinium, or 4-methylpyridinium salts using  $\text{BF}_4^-$  as counteranion in  $\text{CD}_2\text{Cl}_2$  at 180 K. The reason is presumably signal broadening by intermolecular hydrogen-bond exchange.

In a non- $^1\text{H}$ -decoupled  $^{15}\text{N}$  NMR spectrum of an equimolar solution of **1** and  $^{15}\text{N}$ -enriched  $\text{DMAP-H}^+\text{BF}_4^-$  a singlet was observed at 180 K, as depicted in Figure 3a. The signal is shifted to  $-80$  ppm with respect to the neutral DMAP. It is unlikely that this shift is caused by a hydrogen bond or protonation because the corresponding  $^1\text{H}$  spectrum of the same sample does not contain any signal typical for the mobile proton. Moreover, the observed  $^{15}\text{N}$  signal does not exhibit any scalar coupling with the bound proton. Therefore, the observed signal is assigned to DMAP, which has formed a covalent bond to Zn, that is, to the species  $[\text{Zn}-\text{DMAP}]$  (Figure 3a). Complexes of this type have been reported in the past.<sup>50,51</sup>

By contrast, the  $^{15}\text{N}$  NMR spectrum of an equimolar solution of **1** and  $\text{ColH}^+\text{BARF}^-$  depicted in Figure 3b exhibits at 180 K a doublet with a coupling constant of  $|^1J(^1\text{H}, ^{15}\text{N})| = 75$  Hz, shifted by  $-87$  ppm to high field from the signal of the neutral Col. The coupling constant is the same as in the  $^1\text{H}$  NMR spectrum in Figure 2a. It supports the formation of **3** according to Scheme 2. Both the chemical shift and the coupling constant values<sup>52–54</sup> indicate that the proton is located closer to nitrogen than to oxygen, and that it is involved in a strong hydrogen bond.

The  $^{15}\text{N}$  spectrum of **5** at 180 K is depicted in Figure 3c. A broad doublet shifted to  $-104$  ppm as compared to the neutral Col is observed, exhibiting a coupling constant of  $|^1J(^1\text{H}, ^{15}\text{N})| = 90$  Hz, which is masked in the  $^1\text{H}$  NMR spectrum. This finding indicates that the dynamic exchange in which the proton is involved only modulates the  $^1\text{H}$  chemical shift, but not the  $^{15}\text{N}$  one. Similar effects have been described previously.<sup>42,55</sup> The value of the coupling constant indicates a smaller  $\text{N}\cdots\text{H}$  distance in **5** as compared to **3**. Thus, the structure of **5** corresponds to  $\text{Col-H}^+\cdots[(\text{C}_6\text{F}_5)_3\text{BOH}]^-$ .<sup>27</sup>

## DISCUSSION

In this section, we will first discuss the NMR parameters and hence hydrogen-bond properties of the model systems of Schemes 1 and 2 reported in the previous section and relate them to the hydrogen-bond geometries. Then, we will estimate the acidity of the Zn-bound water involved in a direct hydrogen bond to the added bases. Finally, potential implications of our findings for the function of carbonic anhydrase will be discussed.

**Structures of Carbonic Anhydrase Model Systems in an Aprotic Polar Medium.** For Zn-bound hydroxide as a part of the free base **1** (Scheme 1), dissolved in dichloromethane, we found a  $^1\text{H}$  chemical shift of  $-0.5$  ppm at 180 K (Figure 1b). At room temperature no signal could be observed (Figure 1a). We assign this observation to the presence of proton exchange with residual water at room temperature, which precipitates as ice at low temperatures. The chemical shift value of  $-0.5$  ppm compares well with the value of  $-0.06$  ppm found previously for **2**.<sup>32</sup> Here, residual water does not catalyze proton exchange with hydroxide, an observation which we attribute to the large bulky substituents which could hinder the hydroxide-water interaction.

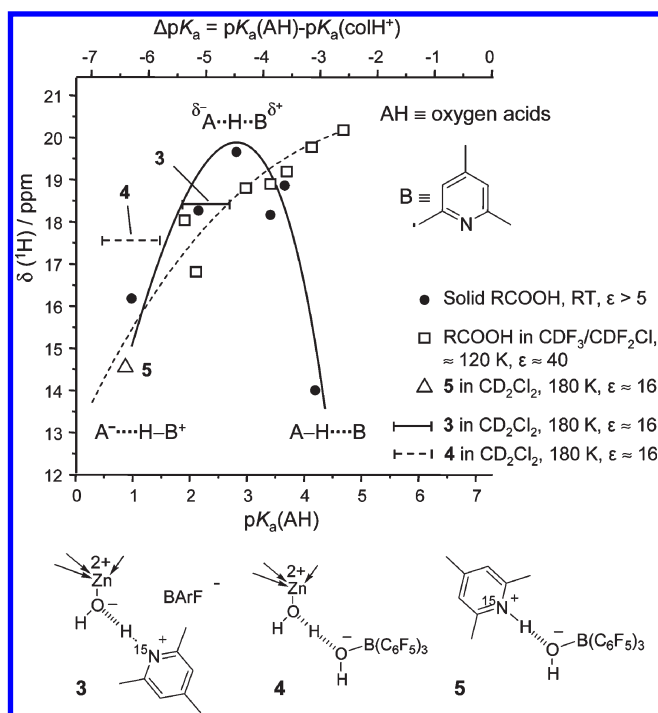


**Figure 4.** The mobile proton chemical shift  $\delta(^1\text{H})$  of collidine–acid complexes in  $\text{CDCl}_3/\text{CDF}_3$  mixture<sup>38</sup> and in the organic solid state<sup>37</sup> as a function of  $\text{pK}_a(\text{HA})$  of the acids and  $\Delta\text{pK}_a = \text{pK}_a(\text{HA}) - \text{pK}_a(\text{ColH}^+)$ .

The hydroxide chemical shifts of **1** and **2** compare well with those of 0.2 ppm found for hydroxyl groups in hydroxyapatite.<sup>56</sup> This demonstrates that Zn-bound hydroxide exhibits similar base properties as free hydroxide. As the latter, the Zn-bound hydroxide then also constitutes an efficient proton acceptor whose ability to form hydrogen bonds with proton donors was explored in the present study.

We were able to identify complex **3** depicted in Scheme 2. The question was whether this complex corresponds to (i) Zn-bound hydroxide forming a hydrogen bond to collidine, (ii) Zn-bound water hydrogen bonded to collidine, or (iii) a situation where the two bases share a proton. This complex was of special interest, because collidine exhibits a similar basicity as the imidazole residue of histidine. In the beginning of our study we used collidinium tetrafluoroborate as acid added to **1** but did not obtain satisfactory results. Only when we replaced  $\text{BF}_4^-$  by the noncoordinating counteranion  $\text{BArF}^-$  were we able to observe complex **3**. The reason is that  $\text{BArF}^-$  does not form hydrogen bonds with proton donors and does not affect the structure of hydrogen-bonded cations in polar organic solution.<sup>42,57</sup>  $\text{BF}_4^-$  also cannot compete with most other proton acceptors for the formation of hydrogen-bonded complexes with added acids. However, it has been experimentally proved that  $\text{BF}_4^-$  remarkably affects the position of the mobile proton of hydrogen-bonded cations.<sup>42</sup> This can facilitate intermolecular hydrogen-bond exchange and prevent the observation of mobile protons by NMR. By contrast, NMR parameters of complex **3** can be identified and correlated with the hydrogen-bond geometries using the NMR hydrogen-bond correlations of collidine complexes with various carboxylic acids established previously, mainly based on dipolar  $^2\text{H}-^{15}\text{N}$  interactions.<sup>37</sup> A comparison of the  $\delta(^1\text{H})$ ,  $\delta(^{15}\text{N})$  and  $^1J(^1\text{H}, ^{15}\text{N})$  values obtained for **3** with

data reported previously<sup>38</sup> allows us—assuming a linear hydrogen bond—to estimate for **3** an average  $\text{O}\cdots\text{N}$  distance of about 2.5 Å and average  $\text{O}\cdots\text{H}$  and  $\text{H}\cdots\text{N}$  distances of about 1.4 and 1.1 Å. Thus, complex **3** exhibits a zwitterionic OHN hydrogen bond of the type  $\text{O}^-\cdots\text{H}\cdots\text{N}^+$ . Using a recent correlation for OHO hydrogen bonds,<sup>49</sup> we estimate for **4** almost the same hydrogen-bond geometry, i.e., an average  $\text{O}\cdots\text{O}$  distance of 2.5 Å and average  $\text{O}-\text{H}$  and  $\text{H}\cdots\text{O}$  distances of 1.1 Å and 1.4 Å. The different  $^1\text{H}$  chemical shift arises from the different properties of N and of O. Later, we will discuss whether the proton is located nearer to Zn or to boron.

**Acidity of the Zn-Bound Water Hydrogen Bonded to a Model Base in an Aprotic Polar Medium.** The finding that H is closer to N than to O in complex **3** indicates that the acidity of Zn-bound water is larger than that of collidinium or that collidine is more basic than Zn-bound hydroxide, under the circumstance that both partners form a direct hydrogen bond in an aprotic polar medium. As some of us have argued in a number of papers in the last years, the discussion of hydrogen-bond geometries constitutes the best way to characterize acid–base properties of hydrogen-bonded complexes.<sup>30,58–61</sup>

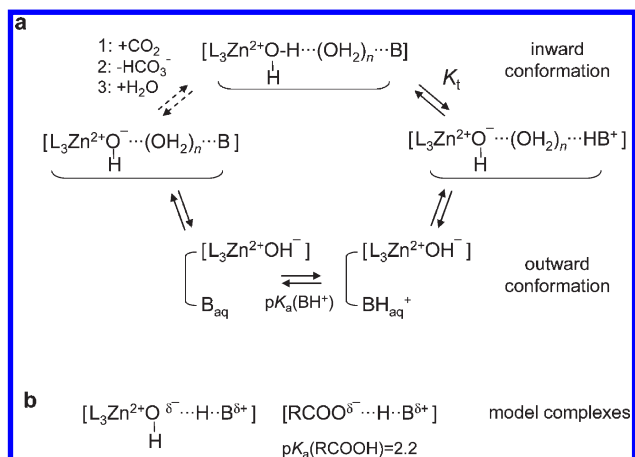
The use of  $\text{pK}_a$  values that refer to an equilibrium between the separate hydrated acids and bases is, therefore, difficult to apply to situations with a direct acid–base contact in the absence of bulk water, as is often the case for active sites of enzymes. We can, however, ask the question which of the many carboxylic acids exhibiting a wide range of  $\text{pK}_a$  values would form with collidine under similar conditions a hydrogen bond of a similar geometry as the Zn-bound water.

For that purpose we have plotted in Figure 4 the  $^1\text{H}$  chemical shifts of various complexes of collidine with carboxylic acids AH as a function of the  $\text{pK}_a(\text{AH})$  values of the acids in water, as well as of the difference  $\Delta\text{pK}_a = \text{pK}_a(\text{AH}) - \text{pK}_a(\text{ColH}^+)$ . The filled circles refer to room temperature data of complexes in the organic solid state<sup>37</sup> and the open squares to complexes around 120 K dissolved in the aprotic polar freon mixture  $\text{CDF}_3/\text{CDF}_2\text{Cl}$ .<sup>38</sup> Correlation lines are included as a guide for the eye, where the solid curve represents the solid-state NMR data and the dashed line the low-temperature liquid state data.

When AH is a weak acid, molecular complexes of the type  $\text{O}-\text{H}\cdots\text{N}$  are formed, where H is located near oxygen. When the acidity of AH is increased, the  $^1\text{H}$  NMR chemical shifts increase because of hydrogen-bond contraction and shift of H toward the hydrogen-bond center, as illustrated by the solid-state data. A maximum chemical shift indicates the formation of a compressed state with a shared proton  $\text{O}^{\delta-}\cdots\text{H}\cdots\text{N}^{\delta+}$ . A further increase of the acidity leads to the zwitterionic form  $\text{O}^-\cdots\text{H}\cdots\text{N}^+$ , where the  $^1\text{H}$  chemical shift is again decreased because the hydrogen bond is widened again. The maximum chemical shift and hence the formation of the shared proton occurs for the solid-state data at  $\Delta\text{pK}_a \approx -4.5$ . This means that the acidity of a neutral oxygen acid and of collidinium are matched in the organic solid state only when the acid in water is stronger by 4.5  $\text{pK}_a$  units as compared to collidinium in water.

The reason for this mismatch is the dielectric permittivity or the constant  $\epsilon$  of the environment. An increase of the local electric fields induces a dipole moment in the hydrogen bond and gives rise to the change of the hydrogen-bond geometries from  $\text{A}-\text{H}\cdots\text{B}$  via  $\text{A}^{\delta-}\cdots\text{H}\cdots\text{B}^{\delta+}$  to  $\text{A}^-\cdots\text{H}\cdots\text{B}^+$ .<sup>30,58,60</sup> Whereas for the organic solid state  $\epsilon < 5$ , the  $\text{CHF}_3/\text{CHF}_2\text{Cl}$  freon mixture exhibits an  $\epsilon$  value of about 40 at 120 K.<sup>30</sup> Therefore, the acidity mismatch is only around  $-2$  in freon

**Scheme 3.** (a) Simplified Catalytic Cycle of CA Reactions of eqs 1 and 2 Derived from Silverman et al.<sup>6</sup> and (b) Schematic Hydrogen Bond Geometries of Model Complexes for CA<sup>a</sup>



<sup>a</sup> L represents organic nitrogen ligands. For further explanation, see the text.

solution as illustrated by the dashed line in Figure 4. In other words, if  $\epsilon$  is increased, the effective acidity of the oxygen acid is increased. The mismatch then disappears for water, where  $\epsilon = 80$ . Finally, we note that for strong acids zwitterionic complexes are always obtained independent of the permittivity, as illustrated by the overlap of the dashed and solid line on the left side of Figure 4.

The data point of 5 [open triangle,  $pK_a(\text{AH}) = 1$ ,  $\Delta pK_a \approx -6.3$ ] in Figure 4 was obtained here at 180 K using CD<sub>2</sub>Cl<sub>2</sub> as solvent, exhibiting at this temperature a dielectric permittivity of  $\epsilon \approx 16$ .<sup>30</sup> The data point is well-located both on the dashed and the solid correlation curves. This means that (C<sub>6</sub>F<sub>5</sub>)<sub>3</sub>BOH<sub>2</sub> behaves in a similar way as a very strong carboxylic acid. In other words, when H is transferred to the base, the chemical constitution of the acid anion residue has a smaller influence on the <sup>1</sup>H chemical shifts as compared to proton shared and molecular complexes.

Let us now come to the discussion of the acidity of Zn-bound water in the model complex 3 in CD<sub>2</sub>Cl<sub>2</sub> at 180 K. The chemical shift obtained,  $\delta(^1\text{H}) = 18.4$  ppm, referring to  $\epsilon \approx 16$ , is symbolized in Figure 4 by a horizontal solid line. The solid line for  $\epsilon < 5$  and the dashed line for  $\epsilon \approx 40$  represent then the margin of error of the estimated acidity of the Zn-bound water. Thus, it follows that 3 exhibits in an aprotic polar environment a proton-donating ability similar to that of a carboxylic acid, which would exhibit in water  $pK_a = 2.2 \pm 0.6$  and  $\Delta pK_a \approx -5$ .

As for (C<sub>6</sub>F<sub>5</sub>)<sub>3</sub>BOH<sub>2</sub>, the value of  $\Delta pK_a$  is  $-6.3$ , and it follows that water bound to boron constitutes a stronger acid than water bound to Zn. Thus, the hydrogen bond proton in 4 will be located closer to the oxygen on Zn than to the oxygen on boron.

It follows that the proton-donating ability of Zn-bound water is unexpectedly large in polar aprotic environment. Whereas the  $pK_a$  of protonated 1 in water/methanol/dichloromethane has been tentatively estimated to be about 6.5,<sup>21,34</sup> in a polar aprotic environment its proton-donating ability is similar to that of a carboxylic acid exhibiting in water a  $pK_a$  value of 2.2.

**Implications for the Catalytic Mechanism of Carbonic Anhydrase.** These results have direct implications in the study of the structure and function of carbonic anhydrase (CA), as

described in the following. In order to address this issue, we present a model of the catalytic mechanism of CA as currently proposed.<sup>6,13</sup> In Scheme 3a we have depicted a simplified catalytic cycle of human carbonic anhydrase II (HCA II) in which L represents histidine residues that are direct ligands of the zinc. B represents the proton-accepting base, i.e., His64 in the wild type. Note that there are many studies using variants of HCA II in which the proton shuttle residue His64 is replaced by a residue such as alanine that is incapable of proton transfer.<sup>11,12,62</sup>

According to this model, catalysis occurs in two separate and distinct stages (a ping-pong mechanism). The first stage comprises the hydration of CO<sub>2</sub>, i.e., addition of CO<sub>2</sub> to Zn-bound hydroxide and the removal of HCO<sub>3</sub><sup>-</sup> accompanied by the addition of water at the Zn. Pentacoordinated Zn complexes are possible intermediates of this process.<sup>63</sup> After this reaction has occurred, the second stage of catalysis is the transport of a proton from the active site to buffers in bulk solvent. A proton of the Zn-bound water cannot directly be ejected into the water phase at a rate sufficient to support the catalytic turnover of 10<sup>6</sup> s<sup>-1</sup>.<sup>64,65</sup> but is transferred in a proton shuttle to the base B.<sup>62,66</sup> This proton transfer in the second stage of catalysis is the rate-limiting event in the maximal velocity of catalysis and is the step associated with substantial H/D kinetic isotope effects of magnitude near 4.<sup>66</sup> There is a pertinent conformational change when the base B is the imidazole side chain of His64. In crystal structures this side chain is observed in inward and outward conformations, corresponding to whether the imidazole of His64 is oriented toward or away from the Zn.<sup>67,68</sup> In the outward conformation, the protonated base of His64 comes into better contact with the bulk solvent into which the proton is ejected.

In the first order,  $K_t$  of Scheme 3 is independent of pH, as in this reaction no proton exchange with the solvent takes place. An indirect dependence is possible, for example induced by protonation–deprotonation processes of nearby amino acid side chains which alter the local electrostatics. For example,  $K_t$  will increase if an anion is created nearby the base B, thus minimizing the Coulomb interaction. However, it is complicated to evaluate  $K_t$  from experimental  $pK_a$  values of Zn-bound water and His64 because it is difficult to differentiate the contributions of the inward and outward conformations. This problem does not occur in computational studies, as  $pK_a$  values are derived from free energy calculations. A correct choice of basis sets and solvation models helps to reproduce the experimental values.<sup>69</sup> Warshel et al.<sup>70</sup> predicted a decrease of the free energy when H is transferred in CA from Zn to histidine, whereas Elstner et al.<sup>15</sup> found a near-degenerate reaction for the isolated model system (His)<sub>3</sub>Zn<sup>2+</sup>(H<sub>2</sub>O)<sub>3</sub>His.

What can our model studies described above contribute to our understanding of the reactions catalyzed by carbonic anhydrase? In Scheme 3b are summarized schematically our results, where we observed a direct acid–base complex between Zn-bound water and collidine B in an aprotic polar solution. Collidine exhibits in water a similar basicity as a histidine imidazole side chain. We observed similar OHN hydrogen-bond geometries for Zn-bound water interacting with collidine as in related complexes with carboxylic acids RCOOH exhibiting in water a  $pK_a$  value of 2.2. For acids with larger values the proton is shifted more to oxygen. This means that in a polar nonaqueous environment the proton-donor ability of Zn-bound water is larger than that of protonated collidine or histidine. By contrast, the  $pK_a$  values of Zn-bound water<sup>2,6,19,20</sup> in aqueous solution which are on the order of 7 are similar to those of the imidazolium side chain of His64.

Our results strongly suggest that a comparison of the  $pK_a$  values obtained in the water phase are not suitable to predict the equilibrium constant of tautomerism in the proton shuttle mechanism, especially in situations in which solvent in the active site has been displaced and the environment is closer to the nonaqueous polar conditions of our NMR results. This is particularly applicable to studies using the variant of HCA II in which His64 is replaced by Ala, and the proton transfer mechanism is sustained using derivatives of imidazole and pyridine.<sup>11,62</sup> In such studies proton transfer may proceed, at least in part, directly between the exogenous acceptor and the zinc-bound water, as opposed to proton transfer through intervening water bridges. In addition, concentrations of the imidazole and pyridine derivatives near 10–50 mM required to sustain proton transfer are likely to further displace water from the active site. In such studies using Ala64, conclusions in previous reports have been obtained based on the values of  $pK_a$  obtained in aqueous solution, and our results here show that this may be inappropriate.

In the case of wild-type HCA II, the inward conformation of His64 displaces at most one or two water molecules in the active-site cavity, and a hydrogen-bonded chain of water molecules intervenes between His64 and the zinc-bound water.<sup>68</sup> In this case, the active-site environment is at least partially solvated with water and the active-site environment can be less like the nonaqueous conditions of our NMR studies, although there is an entire region of the cavity that is lined with hydrophobic residues. As stated above, in the inward conformation the local electrostatics may strongly modify the acid–base properties of Zn-bound water.

## CONCLUSIONS

We have succeeded to observe by NMR hydrogen bonds of Zn-bound water directly interacting with a nitrogen base in polar aprotic solution and compared them with related carboxylic acids. The NMR parameters provide information on the average hydrogen-bond geometries. The nitrogen base used was collidine, which exhibits similar base properties as histidine side chains. In the Zn-bound water–collidine complex we observe the proton near nitrogen. In order to produce a similar hydrogen-bond geometry using a carboxylic acid we find that the latter must exhibit at least a  $pK_a$  value of 2.2 in water. As discussed in the Introduction, our Zn model complexes do not carry a positive charge like the Zn ion in the active site of carbonic anhydrase. The presence of such a charge would then even increase further the acidity of Zn-bound water and hence strengthen the present conclusions.

Although our model systems are very different from the structure of the proton shuttle of carbonic anhydrase, it is hard to decide at the present stage of investigation if they are more or less reliable than  $pK_a$  considerations for predicting the relative acid–base properties of Zn-bound water and histidine in the inward conformation (Scheme 3a). This argument is supported by the recent finding that acid–base hydrogen bonds in active sites of enzymes behave like in polar aprotic solution rather than in water.<sup>28</sup> Future experimental and computational studies will be necessary in order to further corroborate the results described, but we hope that the difference of the acid–base properties of the inward and the outward conformations of carboanhydrase might obtain more experimental and computational attention than before.

## AUTHOR INFORMATION

### Corresponding Author

shender@chemie.fu-berlin.de; limbach@chemie.fu-berlin.de

### Present Addresses

<sup>§</sup>Institut für Organische Chemie, Universität Hannover, Hannover, Germany.

## ACKNOWLEDGMENT

We thank Prof. Dr. Heinrich Vahrenkamp (Albert-Ludwigs-Universität Freiburg, Germany) for providing us with samples of  $[Tp^{R1,R2}ZnOH]$  and Prof. G. S. Denisov, St. Petersburg State University, Russian Federation, for helpful comments. This work was supported by funds provided by the Deutsche Forschungsgemeinschaft, Bonn, and the Russian Foundation of Basic Research (Project 09-03-91336) and the contract 02.740.11.0214.

## REFERENCES

- (1) Hewett-Emmett, D.; Tashian, R. E. *Mol. Phylogenet. Evol.* **1996**, *5*, 50–53.
- (2) Lindskog, S. *Biochemistry* **1997**, *5*, 2641–2646.
- (3) Lindskog, S. *Pharmacol. Ther.* **1997**, *74*, 1–20.
- (4) Supuran, C. T.; Scozzafava, A. *Expert Opin. Ther. Pat.* **2000**, *10*, 575–600.
- (5) Toba, S.; Colombo, G.; Merz, K. M. *J. Am. Chem. Soc.* **1999**, *121*, 2290–2302.
- (6) Mikulski, R. L.; Silverman, D. N. *BBA-Proteins Proteom.* **2010**, *1804*, 422–426.
- (7) Fisher, S. Z.; Kovalevsky, A. Y.; Domsic, J. F.; Mustyakimov, M.; McKenna, R.; Silverman, D. N.; Langan, P. A. *Biochemistry* **2010**, *49*, 415–421.
- (8) Silverman, D. N.; Tu, C.; Chen, X.; Tanhauser, S. M.; Kresge, A. J.; Laipis, P. J. *Biochemistry* **1993**, *34*, 10757–10762.
- (9) Braun-Sand, S.; Strajbl, M.; Warshel, A. *Biophys. J.* **2004**, *87*, 2221–2239.
- (10) Tu, C. K.; Silverman, D. N. *Biochemistry* **1989**, *28*, 7913–7918.
- (11) An, H.; Tu, C.; Duda, D.; Montanez-Clemente, I.; Math, K.; Laipis, P. J.; McKenna, R.; Silverman, D. N. *Biochemistry* **2002**, *41*, 3235–3242.
- (12) Elder, I.; Tu, C. K.; Ming, L. J.; McKenna, R.; Silverman, D. N. *Arch. Biochem. Biophys.* **2005**, *437*, 106–114.
- (13) Silverman, D. N.; McKenna, R. *Acc. Chem. Res.* **2007**, *40*, 669–675.
- (14) Smedarchina, Z.; Siebrand, W.; Fernandez-Ramos, A.; Cui, Q. *J. Am. Chem. Soc.* **2003**, *125*, 243–251.
- (15) Elstner, M.; Cui, Q.; Muni, P.; Kaxiras, E.; Frauenheim, T.; Karplus, M. *J. Comput. Chem.* **2003**, *24*, 565–581.
- (16) Sharif, S.; Shenderovich, I. G.; Gonzalez, L.; Denisov, G. S.; Silverman, D. N.; Limbach, H. H. *J. Phys. Chem. A* **2007**, *111*, 6084–6093.
- (17) Maupin, C. M.; McKenna, R.; Silverman, D. N.; Voth, G. A. *J. Am. Chem. Soc.* **2009**, *131*, 7598–7608.
- (18) Maupin, C. M.; Voth, G. A. *Biochim. Biophys. Acta* **2010**, *1804*, 332–341.
- (19) Kararli, T.; Silverman, D. N. *J. Biol. Chem.* **1985**, *260*, 3484–3489.
- (20) Tu, C.; Qian, M.; Earnhardt, J. N.; Laipis, P. J.; Silverman, D. N. *Biophys. J.* **1998**, *74*, 3182–3189.
- (21) Parkin, G. *Chem. Rev.* **2004**, *104*, 699–767.
- (22) Wooley, P. *Nature* **1975**, *258*, 677–682.
- (23) Slebocka-Tilk, H.; Cocho, J. L.; Frakman, Z.; Brown, R. S. *J. Am. Chem. Soc.* **1984**, *106*, 2421–2431.
- (24) Trofimenko, S. *Chem. Rev.* **1993**, *93*, 943–980.

- (25) Kimura, E.; Kikuta, E. *J. Biol. Inorg. Chem.* **2000**, *5*, 139–155.
- (26) Sakurai, M.; Furuki, T.; Ionue, Y. *J. Phys. Chem.* **1995**, *99*, 17789–17794.
- (27) Andreeva, D. V.; Ip, B.; Gurinov, A.; Tolstoy, P. M.; Denisov, G. S.; Shenderovich, I. G.; Limbach, H. H. *J. Phys. Chem. A* **2006**, *110*, 10872–10879.
- (28) Sharif, S.; Fogle, E.; Toney, M. D.; Denisov, G. S.; Shenderovich, I. G.; Buntkowsky, G.; Tolstoy, P. M.; Chan Huot, M.; Limbach, H. H. *J. Am. Chem. Soc.* **2007**, *129*, 9558–9559.
- (29) Morgan, S. O.; Lowry, H. H. *J. Phys. Chem.* **1930**, *34*, 2385–2432.
- (30) Shenderovich, I. G.; Burtsev, A. P.; Denisov, G. S.; Golubev, N. S.; Limbach, H. H. *Magn. Reson. Chem.* **2001**, *39*, S91–S99.
- (31) Alsfasser, R.; Ruf, M.; Trofimenko, S.; Vahrenkamp, H. *Chem. Ber.* **1993**, *126*, 703–710.
- (32) Ruf, M.; Burth, R.; Weis, K.; Vahrenkamp, H. *Chem. Ber.* **1996**, *129*, 1251–1257.
- (33) Ruf, M.; Vahrenkamp, H. *Inorg. Chem.* **1996**, *35*, 6571–6578.
- (34) Vahrenkamp, H. *Acc. Chem. Res.* **1999**, *32*, 589–596.
- (35) Shenderovich, I. G.; Tolstoy, P. M.; Golubev, N. S.; Smirnov, S. N.; Denisov, G. S.; Limbach, H. H. *J. Am. Chem. Soc.* **2003**, *125*, 11710–11720.
- (36) Mauder, D.; Akcakayiran, D.; Lesnichin, S. B.; Findenegg, G. H.; Shenderovich, I. G. *J. Phys. Chem. C* **2009**, *113*, 19185–19192.
- (37) Lorente, P.; Shenderovich, I. G.; Golubev, N. S.; Denisov, G. S.; Buntkowsky, G.; Limbach, H. H. *Magn. Reson. Chem.* **2001**, *39*, S18–S29.
- (38) Tolstoy, P. M.; Smirnov, S. N.; Shenderovich, I. G.; Golubev, N. S.; Denisov, G. S.; Limbach, H. H. *J. Mol. Struct.* **2004**, *700*, 19–27.
- (39) Bergquist, C.; Bridgewater, B. M.; Harlan, C. J.; Norton, J. R.; Friesner, R. A.; Parkin, G. *J. Am. Chem. Soc.* **2000**, *122*, 10581–10590.
- (40) Jiang, F.; McCracken, J.; Peisach, J. *J. Am. Chem. Soc.* **1990**, *112*, 9035–9044.
- (41) Brookhart, M.; Grant, B.; Volpe, A. F., Jr. *Organometallics* **1992**, *11*, 3920–3922.
- (42) Lesnichin, S. B.; Tolstoy, P. M.; Limbach, H. H.; Shenderovich, I. G. *Phys. Chem. Chem. Phys.* **2010**, *12*, 10373–10379.
- (43) Bergquist, C.; Fillebeen, T.; Morlok, M. M.; Parkin, G. *J. Am. Chem. Soc.* **2003**, *125*, 6189–6199.
- (44) Whaley, T. W.; Ott, D. G. *J. Labelled Compd.* **1974**, *10*, 283–286.
- (45) Golubev, N. S.; Smirnov, S. N.; Schah-Mohammed, P.; Shenderovich, I. G.; Denisov, G. S.; Gindin, V. A.; Limbach, H. H. *Russ. J. Gen. Chem.* **1997**, *67*, 1150.
- (46) Kumar, M.; Singh, S. K. US Patent 2004106801, 2004.
- (47) Gründemann, S. A *Nuclear Magnetic Resonance Study of Proton Transfer Pathways in Transition Metal Complexes*; Mensch & Buch Verlag: Berlin, 2000, pp 33–35.
- (48) Ip, B. C. K.; Andreeva, D. V.; Buntkowsky, G.; Akcakayiran, D.; Findenegg, G. H.; Shenderovich, I. G. *Microporous Mesoporous Mater.* **2010**, *134*, 22–28.
- (49) Limbach, H. H.; Tolstoy, P. M.; Perez-Hernandez, N.; Guo, J.; Shenderovich, I. G.; Denisov, G. S. *Israel. J. Chem.* **2009**, *49*, 199–216.
- (50) Brombacher, H.; Vahrenkamp, H. *Inorg. Chem.* **2004**, *43*, 6054–6060.
- (51) Badura, D.; Vahrenkamp, H. *Inorg. Chem.* **2002**, *41*, 6013–6019.
- (52) Golubev, N. S.; Smirnov, S. N.; Gindin, V. A.; Denisov, G. S.; Benedict, H.; Limbach, H. H. *J. Am. Chem. Soc.* **1994**, *116*, 12055–12056.
- (53) Smirnov, S. N.; Golubev, N. S.; Denisov, G. S.; Benedict, H.; Schah-Mohammed, P.; Limbach, H. H. *J. Am. Chem. Soc.* **1996**, *118*, 4094–4101.
- (54) Limbach, H. H.; Pietrzak, M.; Sharif, S.; Tolstoy, P. M.; Shenderovich, I. G.; Smirnov, S. N.; Golubev, N. S.; Denisov, G. S. *Chem.—Eur. J.* **2004**, *10*, 5195–5204.
- (55) (a) Limbach, H. H. *J. Magn. Reson.* **1979**, *36*, 287–300.  
(b) Limbach, H. H.; Seiffert, W. *J. Am. Chem. Soc.* **1980**, *102*, 538–542.
- (56) Yesinowski, J. P.; Eckert, H.; Rossmant, G. R. *J. Am. Chem. Soc.* **1988**, *110*, 1367–1375.
- (57) Pietrzak, M.; Wehling, J. P.; Kong, S.; Tolstoy, P. M.; Shenderovich, I. G.; Lopez, C.; Claramunt, R. M.; Elguero, J.; Denisov, G. S.; Limbach, H. H. *Chem.—Eur. J.* **2010**, *16*, 1679–1690.
- (58) Golubev, N. S.; Denisov, G. S.; Smirnov, S. N.; Shchepkin, D. N.; Limbach, H. H. *Z. Phys. Chem.* **1996**, *196*, 73–84.
- (59) Sharif, S.; Denisov, G. S.; Toney, M. D.; Limbach, H. H. *J. Am. Chem. Soc.* **2006**, *128*, 3375–3387.
- (60) Ramos, M.; Alkorta, I.; Elguero, J.; Golubev, N. S.; Denisov, G. S.; Benedict, H.; Limbach, H. H. *J. Phys. Chem. A* **1997**, *101*, 9791–9800.
- (61) Limbach, H. H.; Denisov, G. S.; Golubev, N. S. *Hydrogen Bond Isotope Effects Studied by NMR. In Isotope Effects in the Biological and Chemical Sciences*; Kohen, A., Limbach, H.-H., Eds.; Taylor & Francis: Boca Raton FL, 2005; Chapter 7, pp 193–230.
- (62) Tu, C. K.; Silverman, D. N.; Forsman, C.; Jonsson, B. H.; Lindskog, S. *Biochemistry* **1989**, *28*, 7913–7918.
- (63) Miscione, G. P.; Stenta, M.; Spinelli, D.; Anders, E.; Bottoni, A. *Theor. Chem. Acc.* **2007**, *118*, 193–201.
- (64) Lindskog, S.; Coleman, J. E. *Proc. Natl. Acad. Sci. U. S. A.* **1973**, *70*, 2505–2508.
- (65) Khalifah, R. G. *Proc. Natl. Acad. Sci. U. S. A.* **1973**, *70*, 1986–1989.
- (66) Steiner, H.; Jonsson, B. H.; Lindskog, S. *Eur. J. Biochem.* **1975**, *59*, 253–259.
- (67) Nair, S. K.; Christianson, D. W. *J. Am. Chem. Soc.* **1991**, *113*, 9455–9458.
- (68) Fisher, S. Z.; Maupin, C. M.; Budayova-Spano, M.; Govindasamy, L.; Tu, C.; Agbandje-McKenna, M.; Silverman, D. N.; Voth, G. A.; McKenna, R. *Biochemistry* **2007**, *46*, 2930–2937.
- (69) Borstnar, R.; Choudhury, A. R.; Stare, J.; Novic, M.; Mavri, J. *J. Mol. Struct.* **2010**, *947*, 76–82.
- (70) Schutz, C. N.; Warshel, A. *J. Phys. Chem. B* **2004**, *108*, 2066–2075.